Nonresonant carrier transfer in single InGaAs/GaAs quantum dot molecules

Wen-Hao Chang,* Hsuan Lin, Sheng-Yun Wang, Chia-Hsien Lin, Shun-Jen Cheng, and Ming-Chih Lee
Department of Electrophysics, National Chiao Tung University, Hsinchu 300, Taiwan

Wen-Yen Chen and Tzu-Min Hsu
Department of Physics, National Central University, Chung-li 320, Taiwan

Tung-Po Hsieh and Jen-Inn Chyi
Department of Electrical Engineering, National Central University, Chung-li 320, Taiwan
(Received 1 April 2008; revised manuscript received 15 May 2008; published 13 June 2008)

We present a spectroscopic study of single quantum dot molecules (QDMs) formed by two closely stacked $In_{0.5}Ga_{0.5}As$ layers. The exciton fine structures as well as direct and indirect excitonic species associated with QDMs were identified by power dependent and polarization resolved microphotoluminescence measurements. As the temperature was increased, a directional energy transfer between the direct and indirect excitons in single QDMs was observed. A rate-equation model was developed to explain our data. We show that a phonon-assisted nonresonant tunneling of the hole between the two adjacent dots is responsible for such directional energy transfers in QDMs.

DOI: 10.1103/PhysRevB.77.245314 PACS number(s): 78.67.Hc, 78.55.Cr

The underlying atomlike properties of single semiconductor quantum dots (QDs) are essentials of many proposed quantum information applications, such as single-photon sources[1] and quantum logic gates.[2] For further scalability of such applications, building moleculelike structures with controllable coupling is desired. To this end, many researches have focused on the fabrication and optical properties of QD molecules (QDMs) formed by a pair of either vertically stacked[3–8] or laterally aligned[9] self-assembled QDs. Recently, electrical controls of tunnel coupling in single QDMs have been demonstrated by a series of experiments,[3,5–8] in which rich patterns of electric-field-dependent level anticrossings/crossings for different excitonic species were observed when the electron or hole levels were brought into resonance.

Apart from interdot tunneling, dipole-dipole interactions have also been proposed as a dominant source of interdot coupling in QDMs[10,11] when the direct interdot tunneling is largely suppressed between two nonidentical dots. Experimental evidences based on excitation spectroscopy[12,13] and photon correlation measurements[11] have been reported. In particular, a directional energy transfer of exciton between the two adjacent dots was observed and explained in terms of phonon-assisted Fröster processes.[10,11] However, such a directional transfer of carriers could also arise from nonresonant tunneling, which has been reported on ensemble of In(Al,Ga)As asymmetric QD pairs[14,15] and recently on single InP/InGaP QD pairs.[16] Therefore, it is important to clarify whether the Förster transfer or the nonresonant tunneling is responsible for the directional energy transfer in QDMs.

Here we present a spectroscopic study of single QDMs formed by a pair of closely stacked $In_{0.5}Ga_{0.5}As$ QDs. Fine structures of direct and indirect excitons associated with QDMs were investigated by power dependent and polarization resolved microphotoluminescence (μ-PL) measurements. A directional energy transfer from a direct to an indirect exciton in single QDMs was found as the temperature was increased. This phenomenon is explained in terms of a thermally activated tunneling of the hole between the two adjacent QDs.

The samples were grown on a n^+-GaAs (001) substrate by metal-organic chemical-vapor deposition (MOCVD). The layer sequence consists of a 100-nm undoped GaAs buffer layer, followed by a 500-nm $Al_{0.8}Ga_{0.2}As$ layer and an 80-nm GaAs layer grown at 700 °C. The QDMs, formed by a pair of vertically stacked $In_{0.5}Ga_{0.5}As$ QD layers separated by a thin (5 nm) GaAs spacer layer, were then grown at 500 °C. The growth rate and InGaAs coverage were properly controlled,[17] yielding a low QD density of about 10^8–10^9 cm^{-2}. Finally, the sample was capped by an 80-nm undoped GaAs layer at 500 °C. Cross-sectional transmission electron microscopy (TEM) reveals that InGaAs QDs in each layer are lens shaped, with the height and base diameter of $\sim$3 and $\sim$18 nm, respectively. Although the two QD layers were grown under the same conditions, the upper dots are slightly larger than the lower ones due to the influence of strain fields underneath. As shown in Fig. 1(a), the base-to-base distance of the QDM was determined to be 5 nm, corresponding to a barrier thickness of only $\sim$2 nm. Individual QDM spectra were investigated by a μ-PL setup via an aluminum metal mask with arrays of e-beam patterned apertures ($\phi \sim 0.3$ μm). A He-Ne laser beam was focused onto the aperture via a microscope objective (N.A.=0.5). The photoluminescence (PL) signals were analyzed by a 0.75-m grating monochromator combined with a liquid-nitrogen-cooled charge-coupled device (CCD) camera, which yields a resolution-limited spectral linewidth of about 60 μeV. By using the Lorentzian line-shape fitting, the peak position of emission lines can be determined with an accuracy better than 10 μeV.

For initial characterization, a PL spectrum was taken from unmasked regions of the QDM sample, as shown in Fig. 1(b). Apart from the GaAs near-band-edge emissions at about 1520 meV, an intense wetting-layer (WL) peak was observed at 1350 meV. Since the dot density is low, the QDM signals appeared as a low-energy tail of the WL peak.

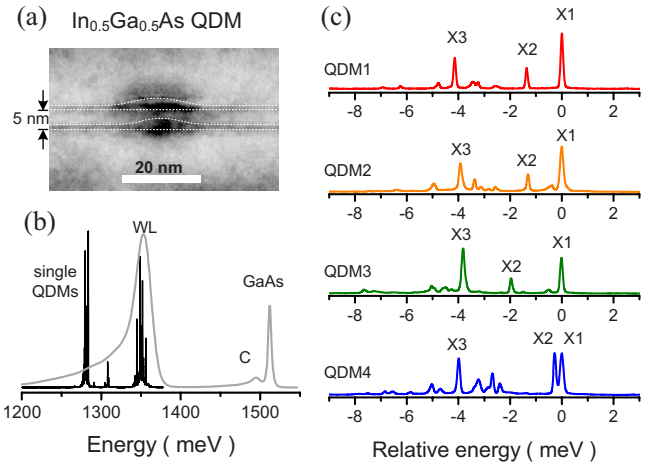

FIG. 1. (Color online) (a) Cross-sectional TEM image of the InGaAs QDM structure. (b) PL spectra for the sample taken from unmasked regions and from one of the fabricated apertures. (c) PL spectra taken from four different QDMs. The energy scale is relative to the $X1$ peak energy at 1283.5, 1285.3, 1257.4, and 1283.8 meV from QDM1 to QDM4, respectively.

Individual QDM spectra were accessed through the fabricated apertures. A typical spectrum taken from one of these apertures is also shown in Fig. 1(b). Single QDM spectra are characterized as a number of sharp lines around ~1280 meV. Several apertures containing only one QDM have been found and five of which have been investigated in detail. All of the investigated QDMs showed similar spectral features. Typical μ-PL spectra for four different QDMs excited nonresonantly under an excitation power of $P_{ex}=2$ μW are displayed in Fig. 1(c). Despite the difference in absolute peak energy, three dominant lines (labeled as $X1$ to $X3$) were observed for all QDMs. The $X1$ and $X2$ lines are separated by an energy ΔE_{12} ranging from 0.3–2 meV for different QDMs, while the $X3$ is almost fixed at about 4.0 ± 0.13 meV below the $X1$ line.

To classify these emission lines, power-dependent PL spectra were measured. Typical results obtained from one of these QDMs (QDM1) are presented in Fig. 2. With the increasing P_{ex}, the intensities of both $X1$ and $X2$ lines increase linearly, as expected for single exciton recombination. Thus, we ascribe $X1$ and $X2$ to different neutral exciton states of the QDM. The $X3$ line that exhibits a superlinear dependence (slope ≈ 1.3) is assigned to the recombination of negatively charged exciton (X^-) in the QDM. The formation of X^- state is related to the unintentionally doped carbon impurities in the MOCVD grown sample (especially in layers grown at low temperature ~500 °C), leading to preferential captures of more electrons into the QDM under nonresonant excitations. Optical control of the formation of X and X^- states in single QDs via the carbon impurity level has been discussed in previous study.[18] Here it is worthwhile to point out that the energy separation between $X3$ and $X1$ is almost the same for different QDMs. Since the binding energy of X^- is less sensitive to the variation in dot size, the similar binding energy indicates that $X3$ is the negatively charged state of $X1$ in the QDM. Apart from neutral and charged excitons, two emission lines $XX1$ and $XX2$ emerge with quadratic and superlinear (slope ≈ 1.6) power dependencies, indicative of biexciton recombination. Another two rather weak peaks were also observed on the lower energy side of the $XX2$ line. The nature of these features is not clear yet. However, their quadratic power dependence implies that each may also relate to biexciton and/or their charged states.

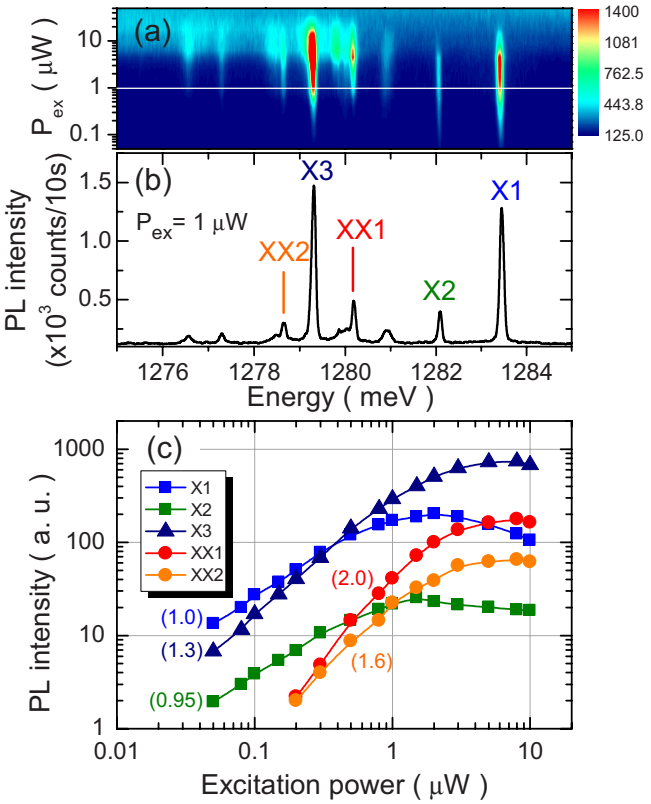

FIG. 2. (Color online) Power-dependent μ-PL spectra of the QDM1 under nonresonant excitations. (a) The contour plot of the PL intensity. (b) The PL spectrum taken at an excitation power of $P_{ex}=1$ μW. (c) The integrated PL intensity of each emission line as a function of P_{ex}. The power dependence of each line is characterized by $I_{PL}\propto P_{ex}^{\alpha}$, with an exponent α shown in parentheses.

The $X1$ and $X2$ lines are unlikely to arise from direct excitons localized in the two different dots because their inherent size difference (~20% according to TEM) would lead to a difference in ground-state energy of at least tens of meV, which cannot account for the variation in the $X1$-$X2$ energy separation ΔE_{12} of just a few meV. Furthermore, for QDMs with spacer thickness of only 5 nm, theoretical calculations predicted that the lowest-lying two electron states hybridize into bonding and antibonding orbitals with an energy separation up to ~50 meV due to the strong interdot tunnel coupling.[19] On the other hand, the lowest-lying two hole states, which are split by only a few millielectron volt, remain essentially uncoupled even in such closely stacked QD pairs, due to the much larger hole effective mass and the interpenetrated strain field.[19] Therefore, the $X1$ and $X2$ lines can be attributed to the recombination of the same electron states with two hole states localized in different dots and characterized as *direct* and *indirect* transitions.

Polarization-resolved PL measurements were employed to further examine the direct and indirect nature of these lines

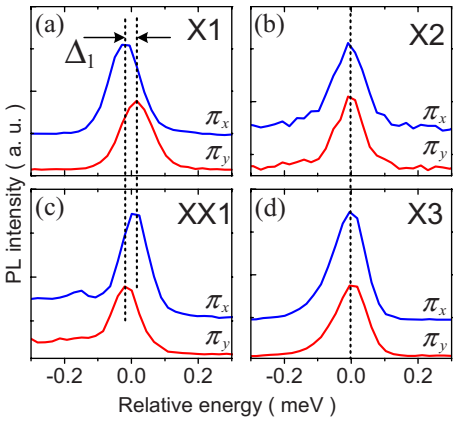

FIG. 3. (Color online) Polarization dependent PL measurements of QDM1.

based on the fine-structure splitting (FSS) in QDMs. In single dots, it has been well established that the electron-hole (e-h) exchange interaction is sensitive to the dot shape symmetry, which splits the neutral exciton line into a linearly cross-polarized doublet.[20,21] The typical FSS is about tens of μeV for InAs dots with linear polarizations along the [110] and [1$\bar{1}$0] directions. For a direct exciton localized in one particular dot, the FSS is expected to resemble the single QD case. However, since the e-h exchange interaction is proportional to the overlap of the electron and hole wave functions, the FSS for an indirect exciton would be decreased substantially due to the reduced wave function overlap. This criterion is helpful in identifying the spatially direct and indirect characters of the observed emission lines. In Fig. 3, linearly polarized spectra of QDM1 along [110] (π_x) and [1$\bar{1}$0] (π_y) directions are displayed. The $X1$ line consists of a linearly cross-polarized doublet with a FSS of $\Delta_1 \approx 30$ μeV. The FSS of $XX1$ is the same as that of $X1$, but with a reversed polarization sequence, indicative of a cascade process for the direct exciton and biexciton in the same dot of the QDM. The $X3$ line exhibits no splitting, as expected for a X^- state where the exchange interaction is quenched by its singlet spin configuration of the two electrons.[21] On the other hand, we found that the FSS of the $X2$ line is virtually zero within our detection limit for all investigated QDMs. Thus, we conclude that $X2$ is the indirect transition.

In order to obtain more information about the interdot coupling, we performed temperature-dependent PL measurements. Figure 4(a) shows such results for QDM1 at T =4.3–24 K under a low-excitation power. With the increasing temperature, the $X1$ intensity (I_1) decreases while the $X2$ intensity (I_2) increases with a crossing in relative intensities $I_{1,2}/(I_1+I_2)$ at T=16 K. As shown in Figs. 4(b)–4(e), the investigated QDMs exhibited a similar behavior but with different crossing temperatures. Because $X1$ and $X2$ are direct and indirect transitions [Fig. 4(f)], the intensity crossing indicates a directional transfer of hole between the two adjacent dots. Such directional transfers are thermally activated processes within time scales comparable to the recombination lifetime of the direct exciton $X1$. To understand the underlying transfer processes, a simplified rate-equation model considering an interdot transfer rate γ_t from $X1$ to $X2$ was used,[10,11]

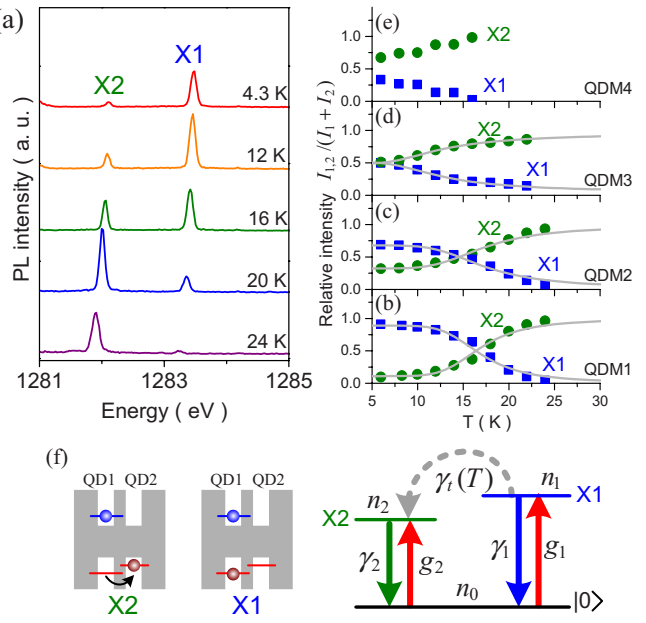

FIG. 4. (Color online) (a) Temperature-dependent PL spectra of QDM1. (b)–(e) The relative intensities of $X1$ and $X2$ transitions, $I_{1,2}/(I_1+I_2)$, as a function of temperature for different QDMs. Solid lines are fitting curves calculated from the rate-equation model. (f) Schematics for the direct and indirect transitions as well as the level diagram of the rate-equation model.

$$\begin{pmatrix} \dot{n}_0 \\ \dot{n}_1 \\ \dot{n}_2 \end{pmatrix} = \begin{pmatrix} -g_1 - g_2 & \gamma_1 & \gamma_2 \\ g_1 & -\gamma_1 - \gamma_t & 0 \\ g_2 & \gamma_t & -\gamma_2 \end{pmatrix} \begin{pmatrix} n_0 \\ n_1 \\ n_2 \end{pmatrix}, \qquad (1)$$

where n_0, n_1, and n_2 are the probability of finding the system to be in vacuum state, $X1$ and $X2$ states; and $g_1(g_2)$ and $\gamma_1(\gamma_2)$ are generation and recombination rates for $X1(X2)$, as schematically shown in Fig. 4(f). For simplicity, biexciton states are neglected in this model, which is applicable under low-excitation conditions. To account for the thermal activation behavior, the temperature dependence of interdot transfer rate was assumed to be $\gamma_t(T)=\gamma_0 \exp(-E_A/k_BT)$, where the γ_0 is a preexponential factor and E_A is the activation energy. Here, the direct coupling between $X1$ and $X2$ has been excluded from this simplified model. In fact, if the two hole levels are directly coupled, the population in the energetically lower-state $X2$ would be significantly higher than that in $X1$ at 4.2 K, since the relaxation bottleneck is not expected for the holes between levels separated by only ΔE_{12}=1.3–2 meV.[22–24] For the investigated QDMs, $I_2 \lesssim I_1$ was typically observed at low temperatures (except QDM4), indicating that the two hole levels are not directly coupled. On the other hand, because the typical coupling strength of direct hole tunneling is $\lesssim$1 meV for barrier thickness $\gtrsim$4 nm (Ref. 25), it can be inferred that the hole levels of the two dots are not aligned and hence suppressing the direct hole tunneling.[26]

By solving the rate equation in steady state, the relative intensity of $X1$ is given by

TABLE I. Fitting parameters E_A, (γ_0/γ_1), and (g_1/g_2) for different QDMs. The energy separation ΔE_{12} between $X1$ and $X2$ are also listed for comparison.

QDMs	ΔE_{12} (meV)	E_A (meV)	γ_0/γ_1	g_1/g_2
1	1.36	10	920	8.0
2	1.30	7.5	140	2.1
3	1.97	3.4	17	1.0
4	0.27	-	-	-
5	1.88	5.0	60	2.1

$$\frac{I_1}{I_1+I_2}=\frac{g_1/(g_1+g_2)}{1+(\gamma_0/\gamma_1)\exp(-E_A/k_BT)}. \quad (2)$$

The relative intensity of $X2$ can then be obtained from $1-[I_1/(I_1+I_2)]$. The advantage of analyzing the relative intensities $I_{1,2}/(I_1+I_2)$, instead of absolute intensities $I_{1,2}$, is that only three fitting parameters are necessary to reproduce the experimental data. The parameters (γ_0/γ_1), E_A, and (g_1/g_2) determine the crossing temperature, the slope of intensity variation with temperature, and the intensity ratio I_1/I_2 at low temperatures,[26] respectively. As shown in Fig. 4, a good agreement is found between the simple model calculation and the experimental data. As for QDM4, the $X2$ intensity is already stronger than $X1$ at the lowest temperature; no intensity crossing can be observed at elevated temperatures. This indicates that the hole levels in QDM4 are directly coupled at low temperatures, as can be inferred from the very small energy detuning of only $\Delta E_{12}\sim 0.3$ meV.

In Table I, the fitting parameters for different QDMs are listed, together with their energy separation ΔE_{12} between $X1$ and $X2$. The fitted values of E_A, (γ_0/γ_1), and (g_1/g_2) did not show noticeable correlation with ΔE_{12}. However, we found that the γ_0/γ_1 shows an exponential dependence on E_A. This can be explained by a thermally activated tunneling of the hole from one dot to another, as schematically illustrated in Fig. 5(a). The hole in QD1 first absorbed the thermal energy (E_A) and is activated to a higher-lying hole level, and then it is tunneled into QD2 followed by rapid relaxations to form an indirect exciton $X2$. For a square tunneling barrier, the interdot tunneling rate can be approximated by

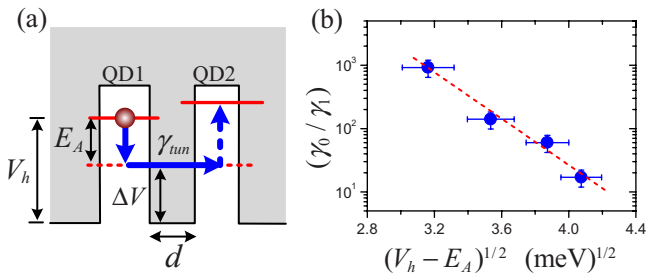

FIG. 5. (Color online) (a) Schematic processes for the thermally activated tunneling of hole between the two adjacent QDs. (b) A semilog plot of the fitted value of γ_0/γ_1 for different QDMs as function of $(V_h-E_A)^{1/2}$, where $V_h=20$ meV.

$\gamma_{tun}\propto\exp[-2d\sqrt{(2m_h^*\Delta V/\hbar^2)}]$, which increases exponentially with the reducing barrier height ΔV and thickness d. This explains why the interdot hole transfer can be considerably enhanced by the absorption of thermal energy (acoustic phonons) to available higher-lying levels, because from which the tunneling barrier height is effectively reduced. Quantitatively, the total transfer rate γ_t via such a thermally activated tunneling is determined by the product of γ_{tun} and the thermionic emission rate. Therefore, the preexponential factor γ_0 in Eq. (2) would involve γ_{tun}, i.e., $\gamma_0\propto\gamma_{tun}$. Figure 5(b) shows a semilogarithmic plot of the fitted γ_0/γ_1 for different QDMs to the estimated $\sqrt{\Delta V}$, where $\Delta V=(V_h-E_A)$ and $V_h=20$ meV were used.[27] Such an exponential dependence clearly demonstrates that the directional energy transfer is a thermally activated tunneling, rather than direct tunneling or dipole-dipole Förster transfers.

For QDMs formed by two nonidentical dots with noticeably different sizes, the direct excitons in different dots would have a large energy difference, which can substantially suppress the dipole-dipole interactions. Even though a phonon-assisted Förster transfer was taken into account,[10,11] i.e., the two direct excitons in different dots were brought into resonance via absorption of thermal energy, the deduced γ_0 should be independent of E_A and should reflect the strength of dipole-dipole interaction, which depends only on the interdot separation and cannot account for the observed exponential dependence of γ_0 on $\sqrt{\Delta V}$.

Our results have an important implication for the control of interdot coupling in a QDM. Electric-field tuning of interdot tunnel coupling was the most successful. However, our results indicated that the thermally activated tunneling of the hole opens another channel for interdot coupling at elevated temperatures, even though the two ground hole levels are detuned from resonance. This would make the electric-field tuning of interdot coupling between hole levels become less controllable, particularly at higher temperatures. Such a thermally activated tunneling would be less significant between electron levels because the confined potential and the interlevel spacing of electron levels are usually significantly larger than that of hole levels.

In summary, we presented a spectroscopic study of single QDMs formed by two closely stacked $In_{0.5}Ga_{0.5}As$ QD layers. The exciton fine structures, as well as direct and indirect excitonic species associated with QDMs, were identified by power dependent and polarization resolved microphotoluminescence measurements. As the temperature was increased, a directional energy transfer between the direct and indirect excitons in single QDMs was observed. A rate-equation model was developed to explain our data. We showed that the origin of the directional energy transfers in QDMs is a thermally activated tunneling of the hole between the two adjacent dots, rather than a direct tunneling or dipole-dipole Förster transfers. Such a nonresonant carrier transfer should be considered in the control of hole level coupling in QDMs at higher temperatures.

This work was supported in part by the program of MOE-ATU and the National Science Council of Taiwan under Grant No. NSC-96–2112-M-009–014.

*whchang@mail.nctu.edu.tw

[1] P. Michler, A. Kiraz, C. Becher, W. V. Schoenfeld, P. M. Petroff, L. Zhang, E. Hu, and A. Imamoglu, Science **290**, 2282 (2000); M. Pelton, C. Santori, J. Vučković, B. Zhang, G. S. Solomon, J. Plant, and Y. Yamamoto, Phys. Rev. Lett. **89**, 233602 (2002); Z. Yuan, B. E. Kardynal, R. M. Stevenson, A. J. Shields, C. J. Lobo, K. Cooper, N. S. Beattie, D. A. Ritchie, and M. Pepper, Science **295**, 102 (2002); W.-H. Chang, W.-Y. Chen, H.-S. Chang, T.-P. Hsieh, J.-I. Chyi, and T.-M. Hsu, Phys. Rev. Lett. **96**, 117401 (2006).

[2] X. Li, Y. Wu, D. Steel, D. Gammon, T. H. Stievater, D. S. Katzer, D. Park, C. Piermarocchi, and L. J. Sham, Science **301**, 809 (2003).

[3] H. J. Krenner, M. Sabathil, E. C. Clark, A. Kress, D. Schuh, M. Bichler, G. Abstreiter, and J. J. Finley, Phys. Rev. Lett. **94**, 057402 (2005).

[4] G. Ortner, M. Bayer, Y. Lyanda-Geller, T. L. Reinecke, A. Kress, J. P. Reithmaier, and A. Forchel, Phys. Rev. Lett. **94**, 157401 (2005).

[5] H. J. Krenner, E. C. Clark, T. Nakaoka, M. Bichler, C. Scheurer, G. Abstreiter, and J. J. Finley, Phys. Rev. Lett. **97**, 076403 (2006).

[6] E. A. Stinaff, M. Scheibner, A. S. Bracker, I. V. Ponomarev, V. L. Korenev, M. E. Ware, M. F. Doty, T. L. Reinecke, and D. Gammon, Science **311**, 636 (2006); M. F. Doty, M. Scheibner, I. V. Ponomarev, E. A. Stinaff, A. S. Bracker, V. L. Korenev, T. L. Reinecke, and D. Gammon, Phys. Rev. Lett. **97**, 197202 (2006).

[7] M. Scheibner, M. F. Doty, I. V. Ponomarev, A. S. Bracker, E. A. Stinaff, V. L. Korenev, T. L. Reinecke, and D. Gammon, Phys. Rev. B **75**, 245318 (2007).

[8] M. Scheibner, I. V. Ponomarev, E. A. Stinaff, M. F. Doty, A. S. Bracker, C. S. Hellberg, T. L. Reinecke, and D. Gammon, Phys. Rev. Lett. **99**, 197402 (2007).

[9] G. J. Beirne, C. Hermannstädter, L. Wang, A. Rastelli, O. G. Schmidt, and P. Michler, Phys. Rev. Lett. **96**, 137401 (2006).

[10] A. O. Govorov, Phys. Rev. B **71**, 155323 (2005).

[11] B. D. Gerardot, S. Strauf, M. J. A. de Dood, A. M. Bychkov, A. Badolato, K. Hennessy, E. L. Hu, D. Bouwmeester, and P. M. Petroff, Phys. Rev. Lett. **95**, 137403 (2005).

[12] S. Yamauchi, K. Komori, I. Morohashi, K. Goshima, T. Sugaya, and T. Takagahara, Appl. Phys. Lett. **87**, 182103 (2005).

[13] H. Gotoh, H. Sanada, H. Kamada, H. Nakano, S. Hughes, H. Ando, and J. Temmyo, Phys. Rev. B **74**, 115322 (2006).

[14] A. Tackeuchi, T. Kuroda, K. Mase, Y. Nakata, and N. Yokoyama, Phys. Rev. B **62**, 1568 (2000).

[15] Yu. I. Mazur, Zh. M. Wang, G. G. Tarasov, Min Xiao, G. J. Salamo, J. W. Tomm, V. Talalaev, and H. Kissel, Appl. Phys. Lett. **86**, 063102 (2005).

[16] M. Reischle, G. J. Beirne, R. Roßbach, M. Jetter, H. Schweizer, and P. Michler, Phys. Rev. B **76**, 085338 (2007).

[17] T.-P. Hsieh, H.-S. Chang, W.-Y. Chen, W.-H. Chang, T. M. Hsu, N.-T. Yeh, W.-J. Ho, P.-C. Chiu, and J.-I. Chyi, Nanotechnology **17**, 512 (2006).

[18] W.-H. Chang, H.-S. Chang, W.-Y. Chen, T. M. Hsu, T.-P. Hsieh, J.-I. Chyi, and N.-T. Yeh, Phys. Rev. B **72**, 233302 (2005).

[19] G. Bester, J. Shumway, and A. Zunger, Phys. Rev. Lett. **93**, 047401 (2004).

[20] M. Bayer, G. Ortner, O. Stern, A. Kuther, A. A. Gorbunov, A. Forchel, P. Hawrylak, S. Fafard, K. Hinzer, T. L. Reinecke, S. N. Walck, J. P. Reithmaier, F. Klopf, and F. Schäfer, Phys. Rev. B **65**, 195315 (2002).

[21] A. Högele, S. Seidl, M. Kroner, K. Karrai, R. J. Warburton, B. D. Gerardot, and P. M. Petroff, Phys. Rev. Lett. **93**, 217401 (2004).

[22] R. Heitz, A. Kalburge, Q. Xie, M. Grundmann, P. Chen, A. Hoffmann, A. Madhukar, and D. Bimberg, Phys. Rev. B **57**, 9050 (1998).

[23] G. Ortner, R. Oulton, H. Kurtze, M. Schwab, D. R. Yakovlev, M. Bayer, S. Fafard, Z. Wasilewski, and P. Hawrylak, Phys. Rev. B **72**, 165353 (2005).

[24] T. Nakaoka, E. C. Clark, H. J. Krenner, M. Sabathil, M. Bichler, Y. Arakawa, G. Abstreiter, and J. J. Finley, Phys. Rev. B **74**, 121305(R) (2006).

[25] A. S. Bracker, M. Scheibner, M. F. Doty, E. A. Stinaff, I. V. Ponomarev, J. C. Kim, L. J. Whitman, T. L. Reinecke, and D. Gammon, Appl. Phys. Lett. **89**, 233110 (2006).

[26] If the two hole levels are not too far away from resonance, a slow direct tunneling rate may contribute to the interdot transfer rate, which will alter the intensity ratio I_1/I_2 at low temperatures. Within our model fitting, this effect has been incorporated into the ratio of generation rates g_1/g_2 so that the direct tunneling component was not included in $\gamma_t(T)$.

[27] The energy difference between the QDM emissions and the WL peak is ~ 70 meV. Adopting a ratio of $V_e:V_h=7:3$ between the electron and hole confined potentials, the hole confined potential is estimated to be $V_h \sim 20$ meV.